An Attempt for Detecting Transonic Buffet Signature via Unsteady-Data Mining

Kazuhisa Chiba*, Shinya Watanabe†, Masaya Nakata‡, Yuhei Umeda§, Naoki Hamada§,
Kanako Yasue¶, Koji Suzuki¶, Shigeru Kuchi-Ishi¶, Kazuyuki Nakakita¶, and Takeshi Ito¶
* Graduate School of Informatics and Engineering
The University of Electro-Communications, Tokyo 182-8585, Japan
Email: kazchiba@uec.ac.jp
† College of Information and Systems
Muroran Institute of Technology, Hokkaido 050-8585, Japan
‡ Faculty of Engineering
Yokohama National University, Yokohama 240-8501, Japan
§ AI Research Center
Fujitsu Laboratories Ltd., Kawasaki 211-8588, Japan
¶ Aeronautical Technology Directorate
Japan Aerospace Exploration Agency, Tokyo 182-8522, Japan

***Abstract*—The transonic buffet degrades the aerodynamic performance of the aircraft during cruise. It is a phenomenon that should be avoided absolutely as it may lead to accidents. However, the mechanism of occurrence has yet to be elucidated. To understand this phenomenon, large-scale unsteady data is accumulated using computational fluid dynamics. In contrast, data mining of time series data such as unsteady data is a topic of the future in that field. In this study, we attempted mining unsteady data with capacity exceeding Tera's order. As a result, the behavior of the physical quantity is suggested to be different from the data just before the transonic buffet occurs. Based on this result, we visualized the data over time, and found that the characteristic change of the viscosity distribution of the blade surface can be seen. This should be a clue to elucidate this phenomenon.**

***Index Terms*—data mining, unsteady aerodynamic data, transonic buffet, sign detection, airplane**

I. Introduction

Unfortunately, the current aircraft has transonic cruises because the supersonic aircraft Concorde has retired because it could not be economically established. Because the shock wave interacts with the separated boundary layer, many transient phenomena occur under transonic flow conditions. The resulting pressure fluctuations cause a number of undesirable unstable effects and therefore there is the possibility of shock wave oscillates known as transonic buffets on the wing surface of the airplane [1].

This is a phenomenon in which the interaction between the shock wave and the turbulent boundary layer and the separation of the flow cause a large self-sustained fluctuation on the profile at the transonic Mach number. Shock-induced variations often lead to periodic impact motion with large amplitude at high subsonic Mach numbers. Although these movements were reported in 1947 [2], the physical mechanism of the wing transonic buffet is still unknown despite the possibility of inducing a severe accident. So the transonic buffet is one of the most important topics in the experimental / computational aerodynamic field. When transonic buffet occurs in a civil aircraft sailing on a daily basis, it is an extremely dangerous phenomenon due to falling into a stall and therefore has a flight profile such that a transonic buffet never occurs. Elucidation of the cause is a matter of great urgency.

Past experiments and calculations show that the transonic buffet phenomenon is low frequency oscillation [3]. It is slower on the order of $\mathcal{O}(10^{-1})$ to $\mathcal{O}(10^{-2})$ than the flow phenomena generated around the wing of the airplane. In recent years, experiments and calculations gradually capture the transonic buffet [4], but its data is enormous in Tera-order due to the fine time scale. Because this is an acceptable quantity as one of Big data [5], it is not possible to easily analyze data for the transonic buffet data set. Big data analysis is a topic in the field of data mining and extensive data analysis, however, in the field of aerospace engineering, it has not been able to successfully use time series data sets such as unsteady aerodynamic data. To acquire knowledge to make use of the design, it is necessary to obtain design information through data mining by effectively using accumulated unsteady data.

The ultimate goal of this project is to reveal the cause of the transonic buffet and to design a new geometry of the airplane wing or a device that does not produce transonic buffet on the aircraft. As a first step, this study defines the origination of the transonic buffet temporally and spatially with respect to a time series data set with a transient phenomenon of transonic buffets constructed by Computational Fluid Dynamics (CFD) To do so, we tried several data mining techniques from conventional to state-of-the-art methods and examined the policy of the next step.

TABLE I
COMPUTATIONAL SCHEMES ON FaSTAR FOR ANALYZING TRANSONIC BUFFET.

Governing equation	Full Navier-Stokes
Discretization	Cell-center
Mesh type	Hybrid
Inviscid flux	Harten-Lax-van Leer-Einfeldt-Wada [7]
Viscous flux	Cell gradient
Gradient evaluation	Weighted Green-Gauss
Limiter	Hishida's limiter
Turbulent model	Spalart-Allmaras (SA-no ft_2-R) [8]
Time integration	Lower/Upper-Symmetric Gauss Seidel [9]
Domain decomposition	METIS
Parallel computation	MPI

II. NUMERICAL METHODS

A. CFD

Unstructured detached eddy simulation (DES) is executed using FaSTAR (FaST Aerodynamic Routines) [6] developed by Japan Aerospace Exploration Agency (JAXA). Summarize the calculation scheme for analyzing the transonic buffet by FaSTAR shown in Table I.

We prepare a calculation model for NACA0012. The 3D model has a length of non-dimensional spanwise length of 0.5 under the dimensionless length chord length of 1.0 shown in Fig. 1. We calculate under the Mach number $M = 0.72$ =const. For data mining, we obtain the data set from dynamic DES analysis (linear angle of attack α sweep from 3.6 to 4.6 [deg] because the transient buffet is predicted from static DES analysis near α of 4.1 [deg]). The initial value of dynamic DES analysis uses the result of static DES and starts contiuation calculation. The dimensionless time step is 0.005 (roughly equivalent to real time 0.003 [s]). We acquire six output data: density ρ, x-directional velocity u, y-directional velocity v, z-directional velocity w, pressure p, and the turbulent eddy viscosity coefficient near the wall $\tilde{\nu}$.

Since the amount of data becomes enormous when physical quantities are acquired in all cells of the mesh, this time we create data sets for data mining at 60 monitoring points. The monitoring points #1 to #30 are on the top side surface of the computational model, and #31 to #60 are set as one layer upper mesh. The monitoring points from #1 to #30 are shown in Fig. 2. The monitoring points from #1 to #10 are on $y = 0.10$, from #11 to #20 are on $y = 0.25$, and from #21 to #30 are on $y = 0.40$. The x coordinates of #1, #11, and #21 are set at $x = 0.05$, #10, #20, and #30 are set at $x = 0.50$. Other monitoring points are set at even intervals.

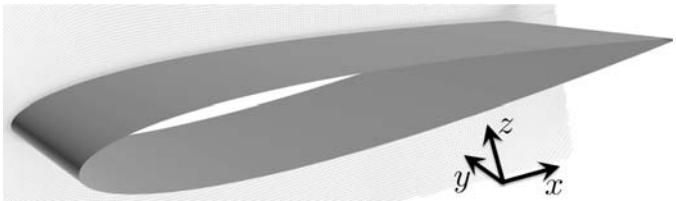

Fig. 1. Computational model using NACA0012. Generated meshes size are $501 \times 101 \times 161$.

B. Data Mining

We employ several data mining techniques: on-demand type correlation-based hierarchical structuring method (CIHSM) [10] including a parallel coordinate plots (PCP) [11] and a scatter plot matrix (SPM) [12], the Barnes-Hut-SNE (Stochastic Neighbor Embedding) [13], and the Betti sequence [14]. CIHSM is a type of rule mining that structures structured rule sets and clarifies organic relationships between rules. Each rule set applies PCP and SPM and examines the physical background generated by the rule set. PCP and SPM are well-known generic tools for visualizing multidimensional data. Although many visualization techniques have been proposed, PCP and SPM are still the method to simply observe the complicated relationship among variables of high dimensional data. Barnes-Hut-SNE is commonly used for visualization of high dimensional data in SPM, and is usually an embedding method executed with $\mathcal{O}(N^2)$.

In contrast, the Betti sequence analysis is based on the chaos theory [15] and the persistent homology [16]; it is one of the topological data analysis (TDA) [17] manners. The Betti sequence is the vector which describes the feature of attractor. It represents the following time evolution equation relative to time series using persistent homology:

$$x_{k+1} = f(x_k,\ x_{k-1},\ \cdots,\ x_1), \tag{1}$$

where x_i ($\forall x_i \in \Re$) denotes time series observations. We analyze the classification scores to cognize the occurrence of buffet via applying the above Betti sequence to unsteady aerodynamic data as TDA viewpoints. The detailed descriptions of the Betti sequence can be referred in [14].

III. RESULTS

A. CFD Result as a Data Mining Dataset

CFD analysis is implemented in JSS2 (JAXA supercomputer system second generation). Dynamic DES analysis takes about two weeks. In this calculation, $alpha$ is shifted from 3.60 to 4.60 [deg]. This is because it was confirmed that the transonic buffet starts from approximately 4.12 [deg] in the result of the static DES calculation separately performed

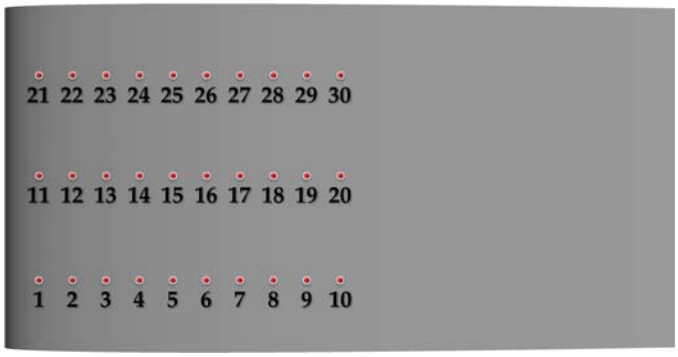

Fig. 2. The monitoring points on the upper surface of NACA0012 computational model.

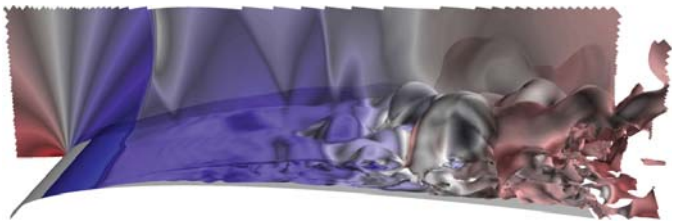

Fig. 3. Instantaneous situation of the CFD result in the transonic buffet on the wing upper region. We illustrate the wing upper surface, iso-surface of turbulent viscosity with C_p distribution, and the surface at $y = 0.40$ with C_p distribution.

(for effective parametric calculation of 2 decimal places, the effective digits are up to 2 decimal places). Analysis of the dynamic DES analysis results showed that the transonic region of transonic buffet is roughly 13% to 24% of the chord length; the Strouhal number S_t on the time scale based on the chord length ($S_t \approx 1$) is approximately 0.073 to 0.081. Thereupon, the current transonic buffet is a low frequent phenomenon.

Figure 3 shows the 3D flow of the instantaneous situation after the transonic buffet began to occur. It consists of an isosurface of the turbulent viscosity with a contour of the pressure coefficient C_p and a calculated surface with $y = 0.40$ with C_p contour. From this figure, we can know the flow structure under transonic buffet condition. Laminar separation occurs behind the shock wave surface. The laminar boundary layer grows, the transition region appears, and the turbulent boundary layer develops. We can also observe three-dimensional nonlinear structure.

B. Data-Mining Result

1) Result from PCP: Dynamic DES data was analyzed from the following viewpoint:

- We compare the changes in the six physical quantities for all monitoring points and find differences in the trends by point.
- We analyze based on two viewpoints:
  - current physical quantities themselves at each monitoring point
  - the difference of physical quantities at each monitoring point at the time before buffet is not still occurring and at the time just before occurrence

  to cognize the difference between that two viewpoints.
- We also compare not only the value of each monitoring point but also the value of data averaged in the surrounding spots and analyze what kind of tendency difference occurs.

As a result, correlation trends between physical quantities are highly dependent on monitoring points. It was found that the nearer the shock wave generation position, the more clear trend is shown. Although it was confirmed that the trend greatly differs depending on the physical quantity and the difference itself, there was no big difference in the strength of the trend between them.

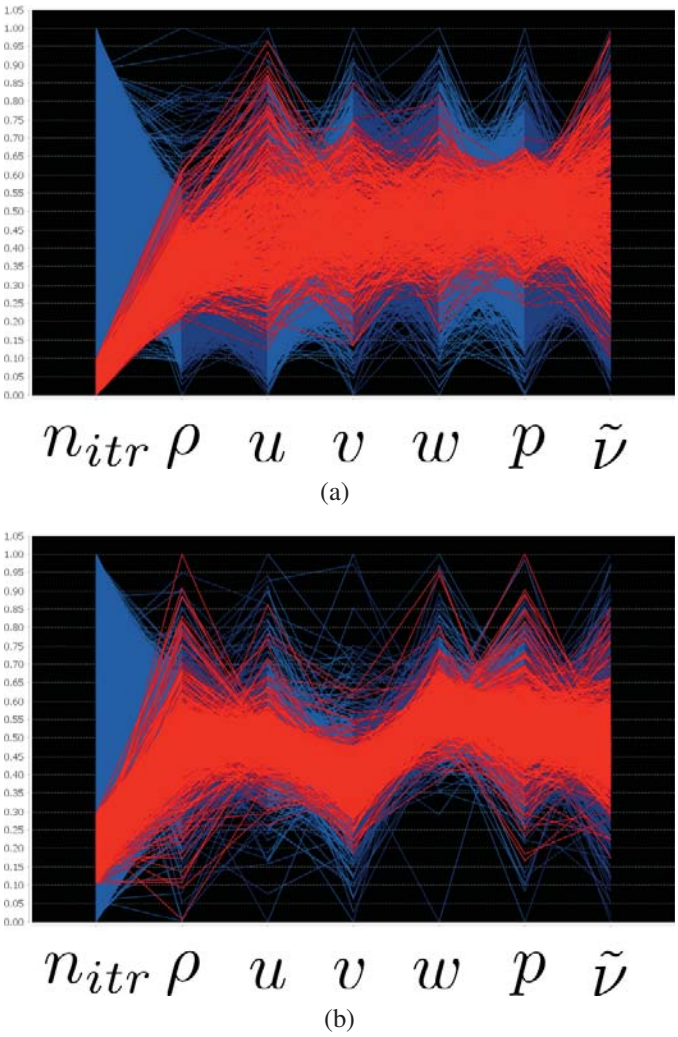

Fig. 4. PCP of averaged sampling difference. (a) the data at the time before occurring transonic buffet. (b) the data at the time immediately before occurring transonic buffet. Note that n_{itr} denotes the computational iteration number.

There are also areas where the trend is strengthened by taking the average of the surrounding monitoring points. A typical monitoring point is #5. Figure 4 shows the PCP of six physical quantities between the time before the transonic buffet occurs and the time just before it occurs. Since this figure shows the difference in behavior of physical quantities which can not be seen in other monitoring points, in the next chapter we visualize the flow structure to clarify the physical reasons different from the others.

2) Result from Barnes-Hut-SNE: Figure 5 shows the result of applying Barnes-Hut-SNE with #01 to #05. The six-dimensional physical quantity shows a dimensionally compressed feature better than expected. Since this algorithm depicts periodic and progressive changes in physical quantities, we expect to visualize time series changes in physical quantities. Classification of physical quantities and examination of trend changes may be applicable to detection of signs. However, even if it seems to be characteristic, it does not

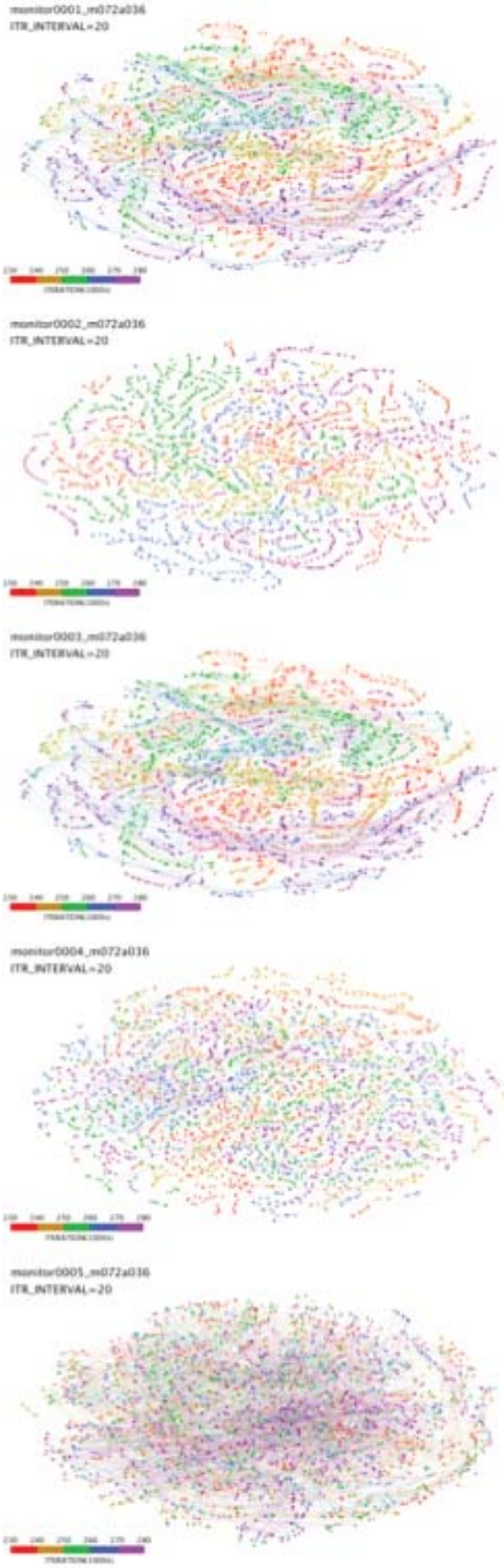

Fig. 5. The result of applying the Barnes-Hut-SNE at the monitoring points from #01 to #05.

indicate which physical quantity should be focused on. Many of the dimensionally compressed features overlap. There are monitoring points that it is difficult to qualitatively comprehend features, but we can not conclude that there is no physical quantity feature, therefore we consider combining with other dimension compression methods.

3) Result from the Betti Sequence: From the analysis results at all monitoring points, the results of #01 to #05 are shown as a representative example in Fig. 6. According to the CFD result, since the position in the chordwise direction is 13

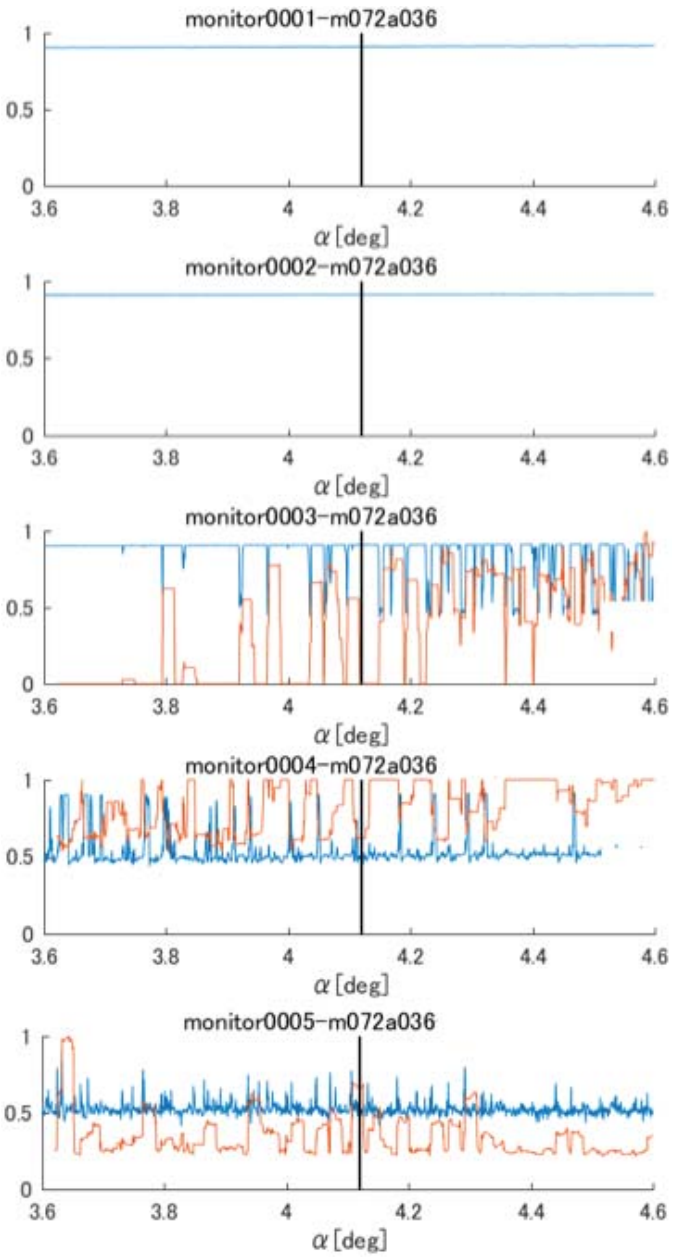

Fig. 6. The result of applying the Betti sequence to u physical quantity at the monitoring points from #01 to #05. Red line describes the normalized number of the Betti sequence and blue line denotes normalized u. The line is drawn at the position at $\alpha = 4.12$ [deg] where transonic buffet was determined to have occurred with the naked eye from CFD animation.

to 24% in the oscillation region of the transonic buffet, the monitoring points #01 and #02 are always located in front of the shock wave regardless of the time. Also, the monitoring points #03 and #04 are in shock wave oscillation, the point #05 always lies behind the shock wave regardless of the passage of time.

For monitoring points #01 and #02, the normal u is a constant value; the Betti sequence value is not detected. In contrast, time series fluctuations are detected at #03 and #04.

Here we need to pay attention to the result of #03. This point is the most anterior position of the chordwise direction where the shock wave oscillation occurs. From the static DES result, it was confirmed that shock wave oscillation begins at α 4.12 [deg], but this result shows the reaction at α 3.7288 [deg]. In the static DES results, it was judged that the attack angle at which the shock wave started to oscillate was the occurrence of a transonic buffet, but in data mining using the Betti sequence, it is suggested that the transonic buffet already started at a lower angle of attack than α 4.12 [deg]. The invisible phenomenon is captured by the Betti sequence, which may be the temporal origination of the transonic buffet.

The time variation of the speed steadily appears at #05, but the value of the Betti sequence rises sharply to α of 3.6202 [deg]. Although no shock wave passes, it is suggested that an abnormal phenomenon occurs behind the shock wave. Due to a phenomenon earlier than α of 3.7288 [deg], which may be a sign of a transonic buffet at #03, the abnormal phenomenon that occurs behind the shock wave may be the beginning of a subsequent transonic buffet. Since we cannot completely deny the possibility that the transonic buffet is already occurring at α of 3.60 [deg], we need to use the sweep calculation result from the angle of attack of less than 3.60 [deg].

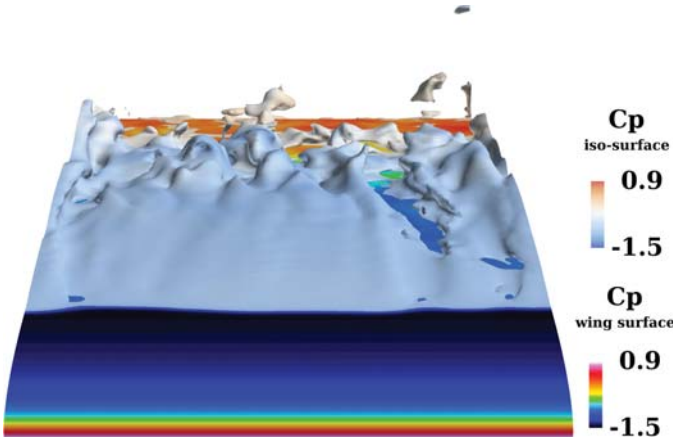

Fig. 7. Front upward visualization of the instantaneous flow structure at the time specified by data mining. Iso-surface of $u = 0$ and C_p distribution on the wing surface.

IV. Feedback of Knowledge from Data Mining to Visualization

A. Observing Flow Structure at the Time Specified by Data Mining

We observe the structure of the instantaneous flow at a specified time to elucidate the anomalies indicated by the PCP and the Betti sequences. Figure 7 shows the frontal upward visualization of the C_p distribution on the wing surface and the isosurface of $u = 0$, which represents the separation boundary of the flow. This figure shows that the separation behavior has three-dimensional nonlinearity with respect to the spanwise direction.

A bird's-eye view is shown in Fig. **??** to clearly show the monitoring points around #5. Figure 8(a) shows that separation behind the shock wave is suppressed near $y = 0$. Separation does not grow and reattaches to the wing upper surface. According to Fig. 8(b), perturbation of C_p on the wing surface

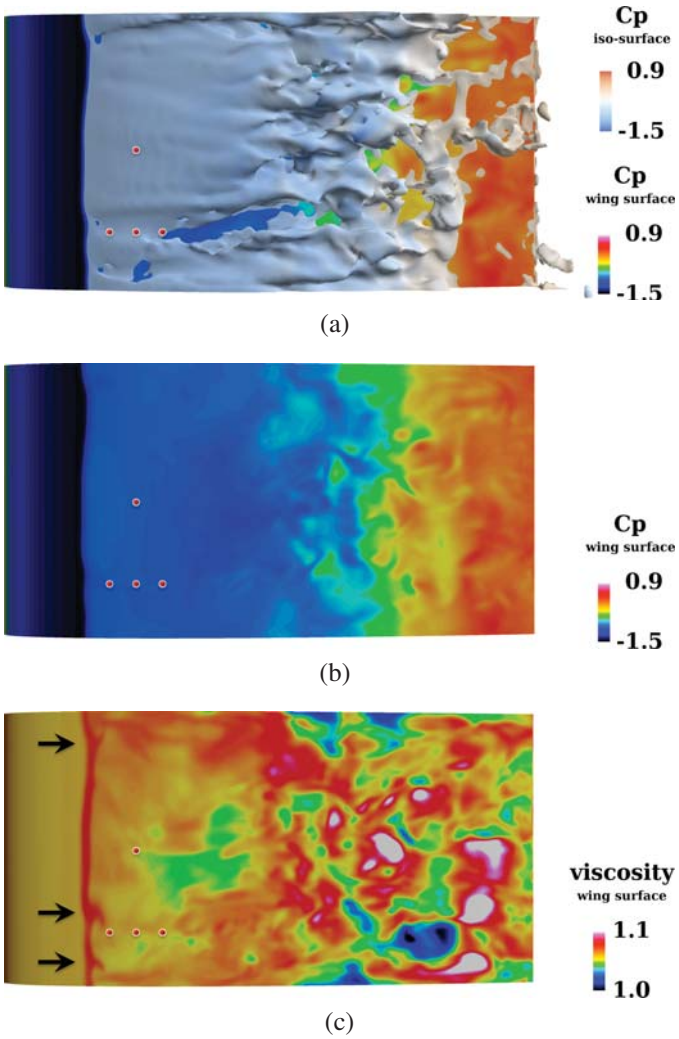

Fig. 8. Upward visualization of the instantaneous flow structure at the time specified by data mining. (a) Iso-surface of $u = 0$ and C_p distribution on the wing surface , (b) just C_p distribution on the wing surface, and (c) Laminar viscosity distribution on the wing surface. Red points denote the monitoring those.

does not appear in the vicinity of #5, but there is a remarkable difference in the spatial structure of x-direction velocity u. Furthermore, in Fig. 8(c) showing the viscosity distribution on the wing surface, three arrows are shown. These are the positions where the highly viscous region is maintained in the chordwise direction. That is, it can be confirmed that the three-dimensional nature of the flow structure with respect to the spanwise direction is generated. High viscosity elongation inhibits separation and causes reattachment. From this result, it is necessary to investigate whether the high viscosity extension phenomenon is a signature of the transonic buffet by preparing not only the data set at the monitoring points near the wing surface but also the monitoring points arranged in the space.

Consequently, Figs. 7 and 8 derived by data mining suggest a physical mechanism to induce three-dimensionality in the span direction. In the PCP having the average difference amount, since the difference of the physical quantity can capture the minute fluctuation, it succeeded in simply grasping the abnormality.

B. Hypothesis regarding Physical Mechanism of Transonic Buffet Outbreak

The consequences of data mining suggest the physical mechanism of transonic buffet as follows;

1) Shock is generated.
2) Pressure fluctuation is generated by shock. (*1)
3) The fluctuation propagates to upstream. (*2)
4) The fluctuation gives an effect on upstream velocity changes; upstream pressure also varies according to the following Rankine-Hugoniot relation:

$$\frac{\rho_2}{\rho_1} = \frac{u_1}{u_2} = \frac{1 + \dfrac{\gamma+1}{\gamma-1}\dfrac{p_2}{p_1}}{\dfrac{\gamma+1}{\gamma-1} + \dfrac{p_2}{p_1}}. \tag{2}$$

   If u_1 decreases, p_1 increases. In contrast, if u_2 swells, p_1 declines.
5) Shock shifts to keep balance in the vicinity of it ? (*3)

To physically explain the above hypothesis, points of doubt are listed below:

- (*1) Why shock yields pressure fluctuation.
- (*2) How pressure fluctuation propagates to upstream. Where is the propagating path. If spatial propagation occurs, spatial monitoring points is necessary.
- (*3) What balance? Circulation?

Further data mining will be performed to give a physical explanation to these in the future.

V. Conclusions

In this study, data mining techniques such as orthodox to state-of-the-art have been applied to large-scale unsteady aerodynamic data on transonic buffets generated by computational fluid dynamics analysis. As a result, several label detection could be performed. Based on this consequence, it was found that the characteristic three-dimensional change of the viscosity distribution of the wing surface can be seen as a result of visualizing the analysis data at the detected time. To investigate the occurrence of the transonic buffet, we found that a more appropriate dataset is necessary, so further data mining, defining the origination of the transonic buffet phenomenon. In addition, by elucidating the physical mechanism, it finally leads to aircraft geometry and devices design that does not cause a transonic buffet.

Acknowledgments

Part of this study was supported by Grant-in-Aid for Scientific Research (C) 16K00295, Japan Society for the Promotion of Science as well as the contract research JX-PSPC-44192 from JAXA. In addition, whole images were created using FieldView16.1 as provided by Intelligent Light via its University Partners Program.

References

[1] B. H. K. Lee, "Self-sustained shock oscillations on airfoils at transonic speeds," *Progress in Aerospace Sciences*, vol. 37, pp. 147–196, 2001.
[2] W. F. Hilton and R. G. Fowler, "Photographs of shock wave movement," 1947, national Physical Laboratories Report & Memoranda No. 2692.
[3] L. Jacquin, P. Molton, S. Deck, B. Maury, and D. Soulevant, "Experimental study of shock oscillation over a transonic supercritical profile," *AIAA Journal*, vol. 47, no. 9, pp. 1985–1994, 2009.
[4] Y. Fukushima and S. Kawai, "Wall-modeled large-eddy simulation of transonic buffet over a supercritical airfoil at high Reynolds number," 2017, aIAA Paper 2017-0495, 2017.
[5] J. Manyika, M. Chui, B. Brown, J. Bughin, R. Dobbs, C. Roxburgh, and A. H. Byers, *Big Data: The Next Frontier for Innovation, Competition, and Productivity*. Mckinsey Global Institute, 2011.
[6] A. Hashimoto, K. Murakami, T. Aoyama, K. Ishiko, M. Hishida, M. Sakashita, and P. R. Lahur, "Toward the fastest unstructured CFD code "FaSTAR"," 2012, aIAA Paper 2012-1075.
[7] S. Obayashi and G. P. Guruswamy, "Convergence Acceleration of an Aeroelastic Navier-Stokes Solver," *AIAA Journal*, vol. 33, no. 6, pp. 1134–1141, 1994.
[8] P. R. Spalart and S. R. Allmaras, "A one-equation turbulence model for aerodynamic flows," 1992, aIAA Paper 92-0439, 1992.
[9] D. Sharov and K. Nakahashi, "Reordering of hybrid unstructured grids for Lower-Upper Symmetric Gauss-Seidel computations," *AIAA Journal*, vol. 36, no. 3, pp. 484–486, 1998.
[10] S. Watanabe, S. Nakano, K. Chiba, and M. Kanazaki, "On-demand correlation-based information hierarchical structuring method (CIHSM) for non-dominated solutions," in *Proceedings on IEEE World Congress on Computational Intelligence*. IEEE, 2016, pp. 1977–1984.
[11] A. Inselberg, "The plane with parallel coordinates," *The Visual Computer*, vol. 1, no. 2, pp. 69–91, 1985.
[12] N. Elmqvist, P. Dragicevic, and J. Fekete, "Rolling the dice: Multidimensional visual exploration using scatterplot matrix navigation," *IEEE Transactions on Visualization and Computer Graphics*, vol. 14, no. 6, pp. 1539–1548, 2008.
[13] L. van der Maaten, "Barnes-Hut-SNE," *CoRR*, vol. abs/1301.3342, 2013. [Online]. Available: http://arxiv.org/abs/1301.3342
[14] Y. Umeda, "Time series classification via topological data analysis," *Transactions of the Japanese Society for Artificial Intelligence*, vol. 32, no. 3, pp. 1–12, D–G72, 2017.
[15] S. Ali, A. Basharat, and M. Shah, "Chaotic invariants for human action recognition," in *Proceedings on IEEE 11th International Conference on Computer Vision*. Rio de Janeiro, Brazil: IEEE, 2007, pp. 1–8.
[16] A. Zomolodian and G. Carlsson, "Computing persistent homology," *Discrete and Computational Geometry*, vol. 33, no. 2, pp. 249–274, 2005.
[17] G. Carlsson, "Topology and data," *Bulletin of the American Mathematical Society*, vol. 46, pp. 255–308, 2009.